ORIGINAL RESEARCH

Targeted Therapy for Hepatocellular Carcinoma: Co-Delivery of Sorafenib and Curcumin Using Lactosylated pH-Responsive Nanoparticles

Yun Bian[1]
Dong Guo[2]

[1]Department of Pharmacy, Affiliated Hospital of Jiangnan University, The Fourth People's Hospital of Wuxi City, WuXi 214000, Jiangsu Province, People's Republic of China; [2]Affiliated Hospital of Jiangnan University, The Fourth People's Hospital of Wuxi City, Wuxi 214000, Jiangsu Province, People's Republic of China

Purpose: Hepatocellular carcinoma (HCC) is a leading cancer worldwide. In the present investigation, sorafenib (SFN) and curcumin (CCM) were co-delivered using pH-sensitive lactosylated nanoparticles (LAC-NPs) for targeted HCC treatment.

Methods: pH-responsive lactosylated materials were synthesized. SFN and CCM co-delivered, pH-responsive lactosylated nanoparticles (LAC-SFN/CCM-NPs) were self-assembled by using the nanoprecipitation technique. The nanoparticles were characterized in terms of particle size, charge and drug release profile. The anti-cancer effects of the nanoparticles were evaluated in human hepatic carcinoma cells (HepG2) cells and HCC tumor xenograft models.

Results: LAC-SFN/CCM-NPs are spherical particles with light coats on the surface. The size and zeta potential of LAC-SFN/CCM-NPs were 115.5 ± 3.6 nm and -34.6 ± 2.4, respectively. The drug release of LAC-SFN/CCM-NPs in pH 5.5 was more efficient than in pH 7.4. LAC-SFN/CCM-NPs group exhibited the smallest tumor volume (239 ± 14 mm^3), and the inhibition rate of LAC-SFN/CCM-NPs was 77.4%.

Conclusion: In summary, LAC-SFN/CCM-NPs was proved to be a promising system for targeted HCC therapy.

Keywords: hepatocellular carcinoma, nanoparticles, pH-responsive, sorafenib, curcumin

Introduction

Hepatocellular carcinoma (HCC) is a leading cancer worldwide.[1] HCC accounts for up to 90% of all primary hepatic malignancies and represents a major international health problem.[2] Due to the increase of the incidence, HCC has become the second leading cause of cancer-related mortality worldwide.[3] Sorafenib (SFN) is the first FDA approved drug as the first-line chemotherapy for the treatment of advanced HCC.[4] Despite the wide clinical application of SFN, its benefits remain modest.[5] Although SFN can prolong the survival of HCC patients, its efficacy is short due to the development of drug-resistant cells.[6] Several strategies have been applied to improve the efficacy of chemotherapeutic agents, such as application of nanoparticle targeted drug delivery systems and combination of two active ingredients.[7]

Nanoparticle platforms loading anti-cancer drugs can prolong the circulation time and facilitate the targeting of drugs to tumors via the enhanced permeability and retention effect.[8] These carriers include polymeric nanoparticles, liposomes, micelles, dendrimers, and so on.[9] The application of nanocarriers in the treatment of HCC is timely and has been recently reviewed.[10] Nanocarriers can be modified with

Correspondence: Dong Guo
Affiliated Hospital of Jiangnan University, The Fourth People's Hospital of Wuxi City, No. 200 Hui He Road, Wuxi 214000, Jiangsu Province, People's Republic of China
Email bianyunjnu@163.com

specific ligands which can assist in targeting and internalization of the drugs to specific cell populations, such as cancer cells.[11] Modification of nanocarriers with saccharides, including galactose, mannose, lactose and maltose, has seen advancement due to their high specificity, low toxicity, low immunogenicity, and a prolonged circulation time.[12] Lactose residue is a promising asialoglycoprotein receptor (ASGPR) targeted ligand due to its high affinity to ASGPR, which is abundantly expressed on hepatocyte membranes, HepG2 cells, and minimally expressed in extrahepatic tissues.[13] So lactosylated nanoparticle is considered as a good targeted system for HCC treatment.[14]

Stimuli-responsive (including reduction, pH, light, and enzyme responsive) nanoparticles were an efficient delivery platform for anticancer drugs, they have many advantages such as improving the availability of drugs and releasing a large number of drugs in response.[15] The extracellular environment of tumors is more acidic than normal tissue, so pH-sensitive nanoparticles are an effective cancer treatment strategy.[16] pH-sensitive nanoparticles could targeted deliver drugs to the tumor zone thus achieving active targeting and overcoming multidrug resistance.[17] In the present study, pH-sensitive lactosylated nanoparticles were constructed for HCC targeted therapy.

Combined chemotherapy is an effective way to treat cancer by reducing side effects and overcoming drug resistance, thus maximizing therapeutic efficacy.[18] Nanoparticle platforms have demonstrated the potential for effective delivery of multiple chemotherapies at tumor sites, enhancing drug half-lives and minimizing free drug toxicity.[19] Co-delivery of two drugs combinations via nanoparticles with synergistic antitumor activities against cancers were wildly developed by researchers.[20–22] Curcumin (CCM) is the active component of Curcuma longa, which is known to inhibit the PI3K/AKT pathway in cancer cells.[23] Curcumin-loaded nanoparticles were reported to enhance cytotoxicity in HCC cells markedly.[24,25] CCM was also co-delivered with other drugs for the combination cancer therapy.[26] Besides the delivery of sorafenib by nanocarriers for HCC therapy,[27,28] the development of combined sorafenib-curcumin loaded-nanoparticles for treatment of HCC is also known in literature.[29] In this research, CCM was co-loaded with SFN to treat HCC.

The present investigation focuses on targeted therapy for HCC. SFN and CCM were co-delivered using pH-responsive lactosylated nanoparticles. Particle size, charge and drug release of nanoparticles were characterized.[30] In human liver cancer cells (HepG2) and liver cancer tumor

transplantation model, the anticancer effect of nanoparticles targeting nanoparticles was studied.

Materials and Methods
Materials
SFN, CCM, lactobionic acid, adipic acid dihydrazide (ADH), dimethyl sulfoxide (DMSO), and 3-(4,5-dimethyl-2-thiazolyl)-2,5-diphenyltetrazolium bromide (MTT) were purchased from Sigma-Aldrich (St Louis, MO). PCL-PEG-CHO was purchased from Shanghai Zzbio Co., Ltd (Shanghai, China). LO2 cells and HepG2 cells were obtained from American Type Culture Collection (Manassas, VA).

Synthesis of pH-Responsive Lactosylated Materials
pH-responsive lactosylated materials were synthesized by conjugating lactobionic acid, ADH, and PCL-PEG-CHO to achieve LAC-ADH-PEG-PCL (Figure 1). Briefly, PCL-PEG-CHO (1 equivalent) and ADH (1 equivalent) were dissolved in DMSO, then triethylamine (1 equivalent) was added and reacted under stirring for 24 h at room temperature to get ADH-PEG-PCL.[31] Lactobionic acid (1.5 equivalents), EDC (1.8 equivalents), and NHS (1.8 equivalents) were dissolved in DMSO and added dropwise to a stirring solution of ADH-PEG-PCL for 3 h at room temperature. LAC-ADH-PEG-PCL was purified dialysis with a dialysis bag and freeze-dried. The IR data of LAC-ADH-PEG-PCL (v/cm^{-1}): 3446 (–OH, –NH–); 2931 (–CH$_2$–, –CH–); 1662 (–HN–CO–, –NH–); 1459 (–CH$_2$CO–); 1093 (–C–O–C–). ^{1}H NMR analysis of LAC-ADH-PEG-PCL showed principal peaks of LAC moiety to be δ 2.02, and 3.49–3.84; ADH moiety of δ 1.57, 2.18, and 8.03; peaks δ 1.86, and 4.08 belong to PEG; δ 1.29, 1.68, and 2.35 are the peaks of PCL chain. ^{1}H NMR spectrum of LAC-ADH-PEG-PCL was provided in Figure 1.

Preparation of SFN and CCM Co-Delivered, pH-Responsive Lactosylated Nanoparticles
SFN and CCM co-delivered, pH-responsive lactosylated nanoparticles (LAC-SFN/CCM-NPs) were self-assembled by using the nanoprecipitation technique.[32–34] Briefly, SFN (50 mg) and CCM (50 mg) were dissolved in acetone (5 mL) (solution 1), LAC-ADH-PEG-PCL (200 mg) was dissolved in ethyl alcohol (10 mL) (solution 2). Then, solution 1 and 2 were added dropwise to deionized water (35 mL) under constant stirring. The organic solvents were evaporated using a rotary evaporator to obtain a free suspension of LAC-SFN/CCM-NPs. The suspension was washed with deionized water
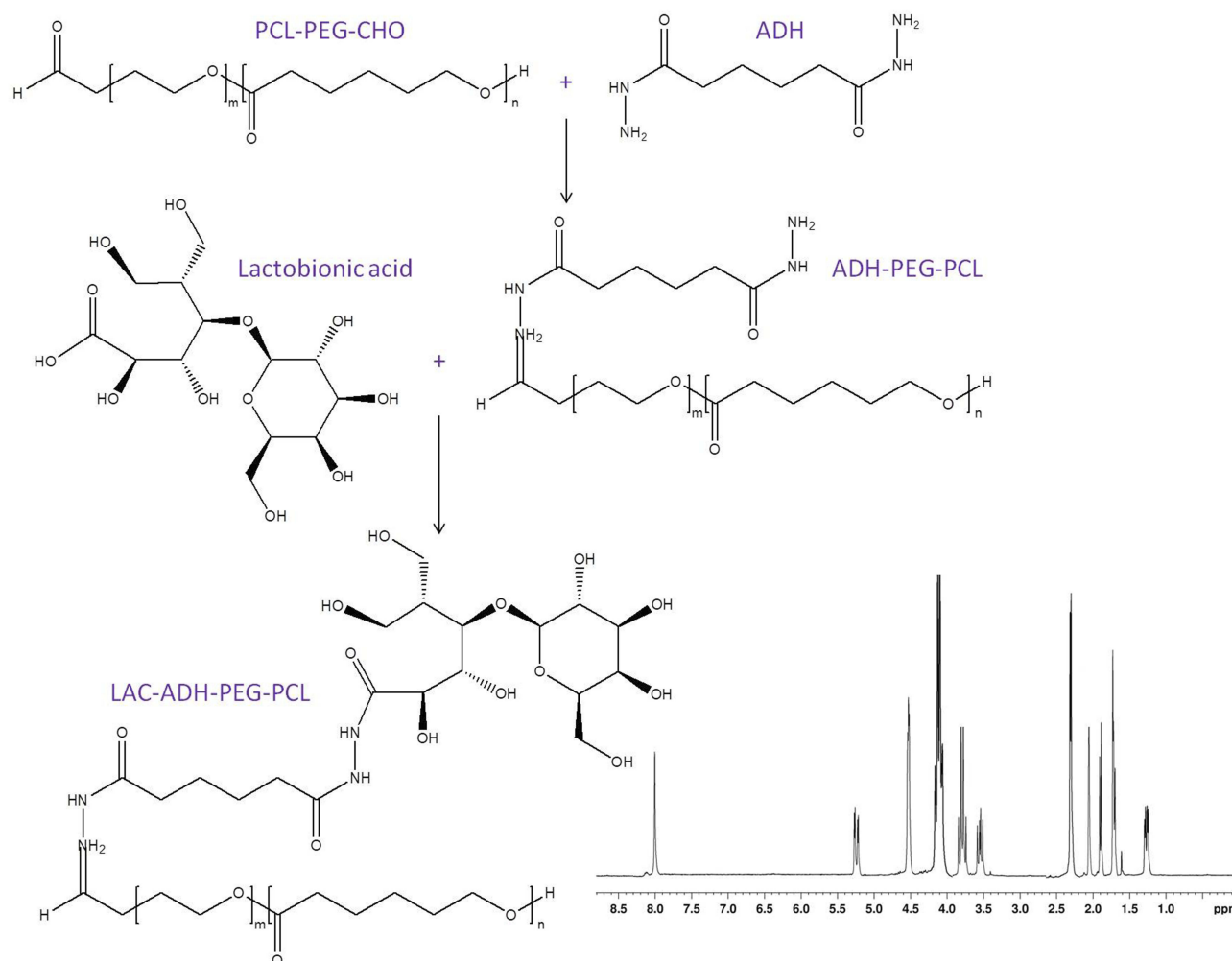
Figure 1 The reaction scheme and ^{1}H NMR spectrum of LAC-ADH-PEG-PCL. LAC-ADH-PEG-PCL were synthesized by conjugating lactobionic acid, ADH, and PCL-PEG-CHO.

several times, filtered using a Millipore filter (0.45 µm) and freeze-dried. Blank pH-responsive lactosylated nanoparticles (LAC-NPs) were prepared by the same procedure without the presence of SFN and CCM. Single SFN or CCM loaded, pH-responsive lactosylated nanoparticles were prepared by the same procedure using SFN (100 mg) or CCM (100 mg) instead of dual drugs combination, named LAC-SFN-NPs and LAC-CCM-NPs. Non-lactosylated nanoparticles (SFN/CCM-NPs) were prepared by the same procedure using PEG-PCL (200 mg) instead of LAC-ADH-PEG-PCL (200 mg).

Characterization of Nanoparticles

The morphology of LAC-SFN/CCM-NPs and SFN/CCM-NPs was detected by transmission electron microscopy (JEM-2100 microscope, JEOL Ltd., Tokyo, Japan). The particle size (mean diameter), size distribution (polydispersity index, PDI) and zeta potential of the obtained nanoparticles

were determined by a Zetasizer Nano ZS (Malvern Instruments, Malvern, UK) operated with dynamic light scattering.[35] Drug entrapment efficiency (EE) and loading capacity (LC) were analyzed using a UV spectrophotometer (Shimadzu, Kyoto, Japan) at 270 nm (for SFN) and 425 nm (for CCM).[36] The EE and LC were calculated by using equations:

$$\text{EE\%} = \text{Amount of drug in nanoparticles} / \text{total amount of drug added} \times 100\% \quad (1)$$

$$\text{LC\%} = \text{Amount of drug in nanoparticles} / \text{amount of drug and excipients} \times 100\% \quad (2)$$

Stability of Nanoparticles

The mean diameter, PDI and EE of LAC-SFN/CCM-NPs, LAC-NPs, LAC-SFN-NPs, LAC-CCM-NPs, and SFN/

CCM-NPs were measured every month for a period of 6 months to determine the stability of the prepared nanoparticles after storage at 2–8°C.[37] The stability of nanoparticles in PBS and culture medium with 10% FBS was also evaluated.

In vitro Release of Nanoparticles

The release manners of SFN and CCM from LAC-SFN /CCM-NPs, LAC-SFN-NPs, LAC-CCM-NPs, and SFN/ CCM-NPs were examined using dialysis method.[38] Briefly, samples were dissolved in phosphate-buffered saline solution (PBS, 5 mL, pH 5.5 or 7.4) and sealed separately in dialysis bags. Samples were dialyzed against 50 mL corresponding buffers, which were incubated in a 37°C water bath under constant shaking (100 rpm). The release medium (2 mL) was taken out at determined time points and replenished with an equal volume of fresh medium. The amount of released SFN and CCM was analyzed using a UV spectrophotometer as described in "Characterization of nanoparticles" section.

In vitro Cytotoxicity and Synergistic Effect

The synergistic effect of the dual drugs loaded nanoparticles was evaluated by comparing the cytotoxicity parameters of LAC-SFN/CCM-NPs, LAC-SFN-NPs, and LAC-CCM-NPs, which were determined using a MTT assay.[39,40] HepG2 cells, sorafenib-resistant cell lines (HepG2/SFN cells), and LO2 cells were seeded in 48-well plates and incubated overnight at 37°C in a 5% CO_2 incubator. LAC-SFN/CCM-NPs, LAC-NPs, LAC-SFN-NPs, LAC-CCM-NPs, SFN/CCM-NPs, and free SFN/ CCM at different drug concentrations were added into each well and incubated for 72 h. Then, MTT solution (20 μL, 5 mg/mL) was added to each well and further incubated for 4 h. Thereafter, the unreacted dye solution was removed, and DMSO solution (200 μL) was added. The absorbance value was measured at 490 nm using a microplate reader. Cell viability and half-maximal inhibitory concentration (IC_{50}) were then calculated for each sample. The synergistic effect was calculated using the combination index (CI) theorem of Chou-Talalay offers quantitative definition for additive effect (CI = 1), synergism (CI < 1), and antagonism (CI > 1) in drug combinations.[41] CI was calculated by the equation: CI_{50} = $C_{SFN}/C_{SFN50} + C_{CCM}/C_{CCM50}$ (3). C_{SFN} and C_{CCM} mean the concentration of SFN and CCM in the combination system at the IC_{50} value. C_{SFN50} and C_{CCM50} represent the IC_{50} value of SFN and CCM, respectively.

Cell Uptake of Nanoparticles

Coumarin 6 was encapsulated into nanoparticles to evaluate the cell uptake efficiency.[42] HepG2 cells were firstly equilibrated with Hank's buffered salt solution at 37°C for 1 h. Then, coumarin 6-loaded nanoparticles (200 mg/mL) were added and incubated for 1, 2, and 8 h. Cells were washed with PBS (1 mL) and photographed by fluorescence microscopy and the cell uptake efficiency was evaluated using a BD FACSCalibur flow cytometer.

Animals

Male BALB/c nude mice (6–8 weeks) were purchased from Beijing Vital River Experimental Animal Technical Co., Ltd (Beijing, China). All the animal experiments were carried out in compliance with the National Institutes of Health guide for the care and use of Laboratory animals (NIH Publications No. 8023, revised 1978) and proved by the Ethics Committee of the Fourth People's Hospital of Wuxi City. HCC tumor xenograft models were established by subcutaneously injecting 2×10^6 HepG2 cells (0.1 mL/ mouse) into the right armpit of the mice.[43]

In vivo Anti-Tumor Efficacy

HCC tumor tumor-bearing mice were randomly assigned to seven groups. LAC-SFN/CCM-NPs (2.5 mg/kg SFN and 2.5 mg/kg CCM), LAC-NPs, LAC-SFN-NPs (2.5 mg/kg SFN), LAC-CCM-NPs (2.5 mg/kg CCM), SFN/CCM-NPs (2.5 mg/kg SFN and 2.5 mg/kg CCM), free SFN/CCM (5 mg/kg SFN and 5 mg/kg CCM), and 0.9% NaCl (control) were intravenously injected to the mice every three days.[44] Tumor size (length and width) was measured using calipers every three days during the treatment. Tumor volumes (TV) were calculated by the equation:[45] TV = the longest axis×the perpendicular shorter axis^2/2 (4). The tumor volume inhibition rate (TIR) on day 21 was calculated by the equation: TIR (%) = (Tumor volume of the control – tumor volume of the treated mice)/tumor volume of the control×100 (5).

In vivo Tissue Distribution

The above HCC tumor tumor-bearing mice which injected with samples were sacrificed by cervical dislocation on 1 and 24 h, the tumor tissue, liver, heart, kidney, lung, and spleen were harvested, washed twice with 0.9% NaCl, weighed, and homogenized.[46,47] The mixture was vortexed for 5 min and centrifugated at 15,000 rpm for 10 min. The amount of released SFN and CCM was analyzed using

a UV spectrophotometer as described in "Characterization of nanoparticles" section.

In vivo Tolerance Analysis

The above HCC tumor tumor-bearing mice which injected with samples were sacrificed by cervical dislocation on days 7, 14, 21 and the blood were collected into heparinized tubes.[48] Blood samples were centrifuged (15,000 rpm for 20 min at 4°C) to isolate plasma and assayed for the alanine transaminase (ALT), creatine phosphokinase (CPK), and lactate dehydrogenase (LDH).

Statistical Analysis

The data of the studies were expressed as the mean ± standard deviation. Statistical analysis was performed using a post hoc test following ANOVA. P values less than 0.05 (*P < 0.05) was considered as statistically significant.

Results

Characterization of Nanoparticles

The TEM images of LAC-SFN/CCM-NPs and SFN/CCM-NPs revealed different morphology. LAC-SFN/CCM-NPs, LAC-SFN-NPs and LAC-CCM-NPs are spherical particles with light coats on the surface, while SFN/CCM-NPs showed uniform particles with smooth surfaces (Figure 2). The IR spectrum of LAC-SFN/CCM-NPs contained peaks at 1550–1750 cm^{-1}, which means the formation of amido acid. It also has the peaks of PEG, PCL and lactose. The size of LAC-SFN/CCM-NPs was 115.5 ± 3.6 nm, which is similar to other lactosylated nanoparticles (LAC-SFN-NPs and so on). However, SFN/CCM-NPs had a diameter of 82.4 ± 2.1 nm, which may be the proof of the lactose modification may increase the particle size. The EE of SFN and CCM was 91.2 ± 2.9 and 83.5 ± 2.1%, indicating the high drug encapsulation efficiency of the nanoparticles. PDI, zeta potential and LC are also summarized in Table 1.
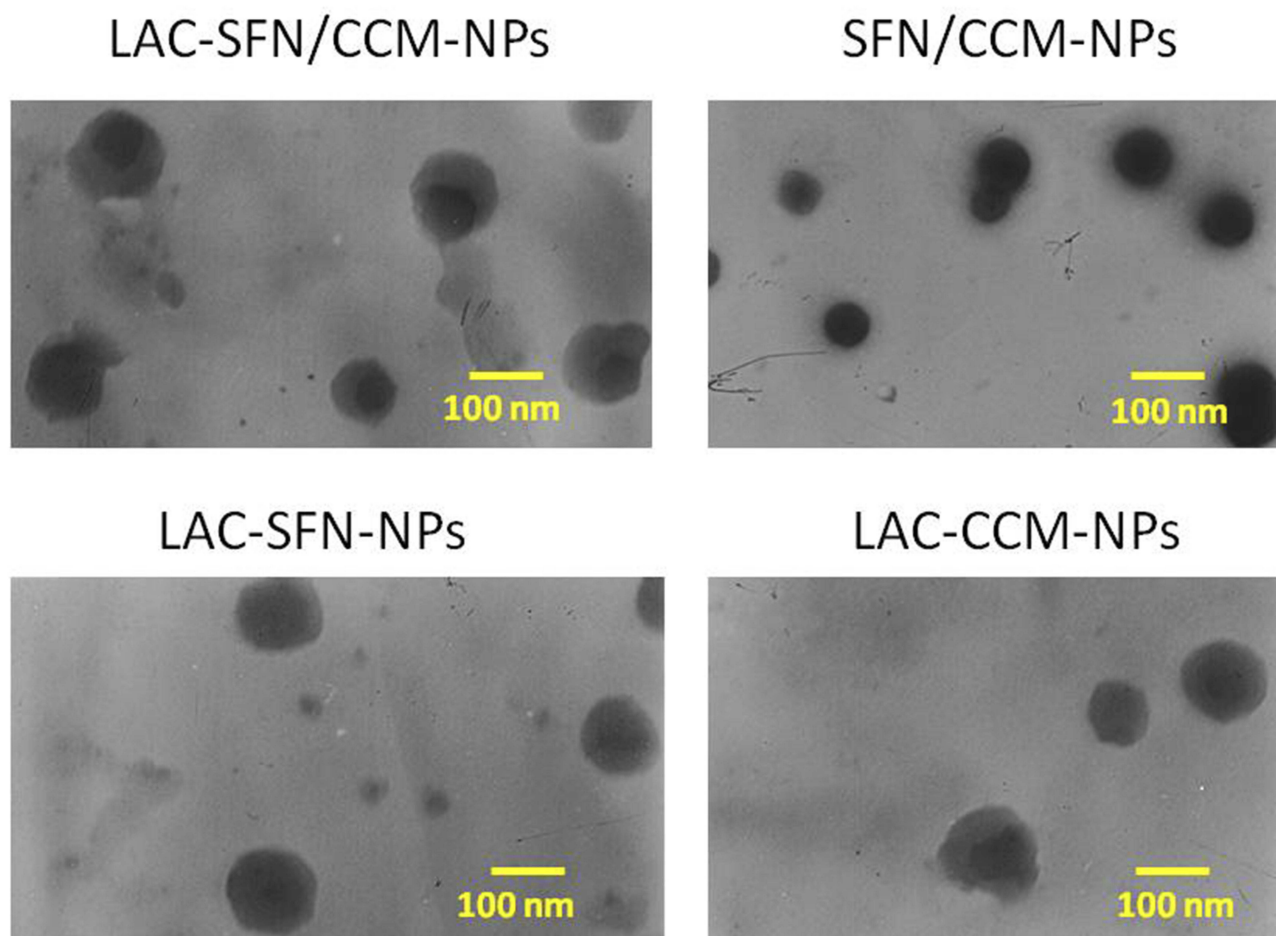

Figure 2 TEM images of LAC-SFN/CCM-NPs, SFN/CCM-NPs, LAC-SFN-NPs, and LAC-CCM-NPs. LAC-SFN/CCM-NPs are spherical particles with light coats on the surface, while SFN/CCM-NPs showed uniform particles with smooth surfaces.

Table 1 Characterization of SLNs (Mean ± SD, n=3)

Formulation	Mean Diameter (nm)	PDI	Zeta Potential (mV)	EE (%)		LC (%)	
				SFN	CCM	SFN	CCM
LAC-SFN/CCM-NPs	115.5 ± 3.6	0.183 ± 0.009	−34.6 ± 2.4	91.2 ± 2.9	83.5 ± 2.1	9.5 ± 0.9	8.9 ± 0.9
LAC-NPs	113.1 ± 2.9	0.152 ± 0.005	−33.1 ± 1.9	/	/	/	/
LAC-SFN-NPs	111.9 ± 2.7	0.137 ± 0.005	−32.8 ± 1.7	89.5 ± 3.1	/	10.3 ± 1.1	/
LAC-CCM-NPs	112.6 ± 3.1	0.171 ± 0.006	−35.1 ± 2.1	/	85.4 ± 2.5	/	9.5 ± 0.8
SFN/CCM-NPs	82.4 ± 2.1	0.126 ± 0.004	−23.1 ± 1.5	90.7 ± 2.7	82.7 ± 2.8	12.6 ± 1.2	10.7 ± 0.7

Stability of Nanoparticles

The nanoparticles systems maintained stable if they showed no obvious changes in size, size distribution, and drug encapsulation efficiency. Figure 3 reveals the particle size, PDI and EE did not change significantly over the period of 6 months, which means the status of the systems remained unchanged during the storage time. The stability of nanoparticles in PBS could last for 96 h, and in cell culture medium with 10% FBS the stability stayed for 72 h.

In vitro Release of Nanoparticles

In vitro release studies of nanoparticles were performed in pH 7.4 and 5.5 to evaluate the pH responsive effect of the systems (Figure 4). The drug release of LAC-SFN/CCM-NPs in pH 5.5 was more efficient than in pH 7.4 ($P <$ 0.05). At the end of the study, over 80% of drugs were released from LAC-SFN/CCM-NPs in pH 5.5, while drugs release in pH 7.4 was less than 60%, indicating the increase of release amount due to hydrolysis of hydrazone. In contrast, non pH-sensitive SFN/CCM-NPs showed no
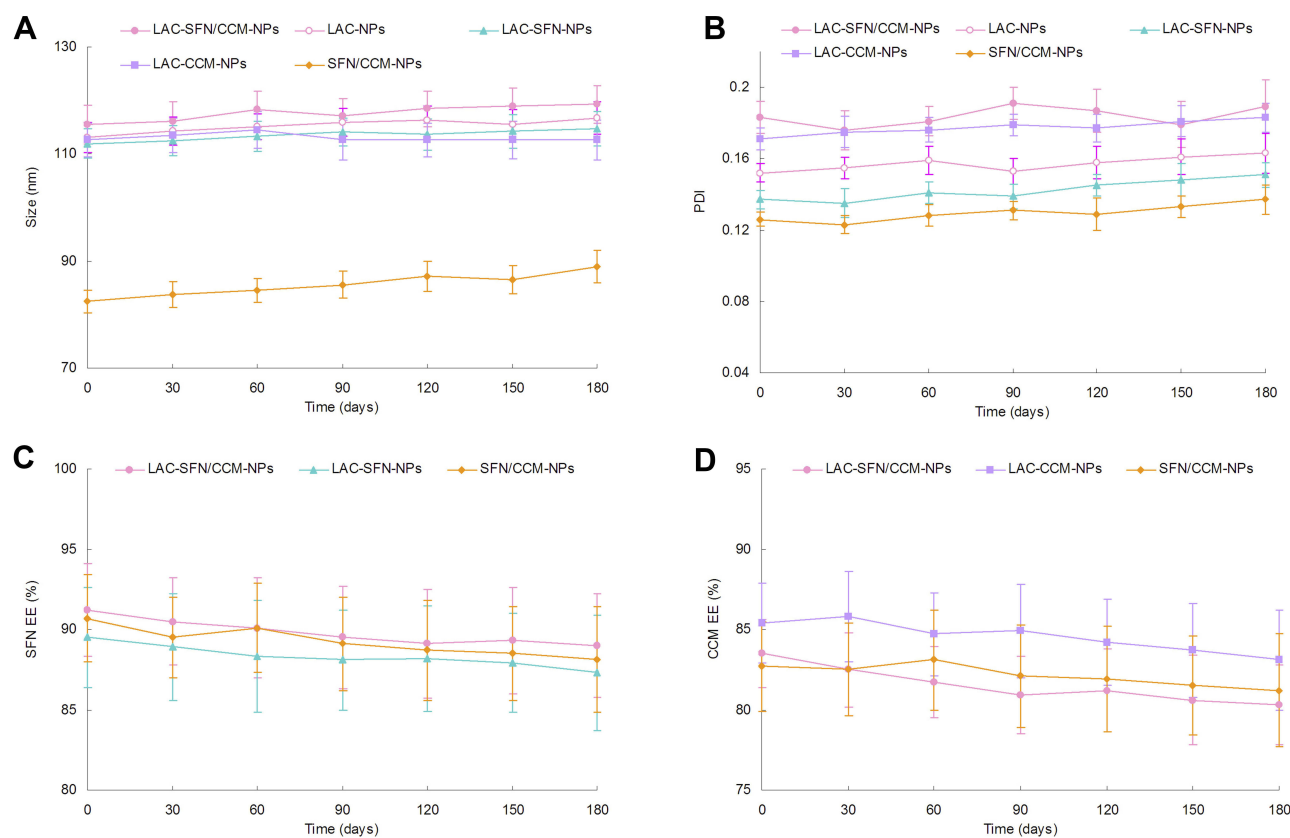

Figure 3 The stability of nanoparticles evaluated by the size (**A**), PDI (**B**), SFN EE (**C**) and CCM EE (**D**) for a period of 6 months. The nanoparticles systems maintained stable if they showed no obvious changes in size, size distribution, and drug encapsulation efficiency.
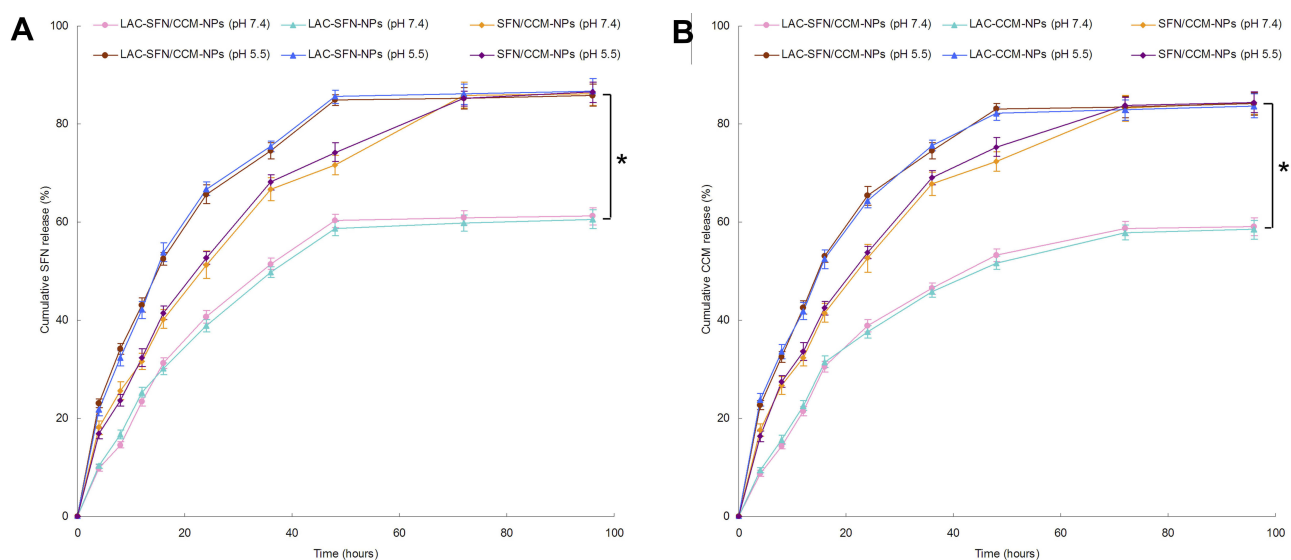
652

Drug Design, Development and Therapy 2020:14

Figure 4 In vitro SFN (**A**) and CCM (**B**) release of nanoparticles preformed in pH 7.4 and 5.5. The drug release of LAC-SFN/CCM-NPs in pH 5.5 was more efficient than in pH 7.4. At the end of study, over 80% of drugs were released from LAC-SFN/CCM-NPs in pH 5.5, while drugs release in pH 7.4 was less than 60%. Data represent mean ± SD, *means P < 0.05.

obvious difference in both pH 7.4 and 5.5. ON the other hand, LAC-SFN/CCM-NPs exhibited slower release rate when compared with non-lactosylated SFN/CCM-NPs, this may be the evidence of the lactose modification on the nanoparticle surface could bring a more sustained release behavior to the system.

In vitro Cytotoxicity and Synergistic Effect

In vitro cytotoxicity of LAC-SFN/CCM-NPs, LAC-NPs, LAC-SFN-NPs, LAC-CCM-NPs, SFN/CCM-NPs, and free SFN/CCM was tested on HepG2 cells. Blank LAC-NPs did not show cytotoxicity and this could prove the low toxicity of the materials in the nano-systems (Figure 5A). Although free SFN/CCM illustrated obvious cytotoxicity, significant improvement in cytotoxicity was obtained by SFN/CCM-NPs (P < 0.05). LAC-SFN/CCM-NPs showed remarkably higher cytotoxicity than SFN/CCM-NPs (P < 0.05), suggested that lactose-modified pH-sensitive ligand could improve the efficiency of the loaded drugs. LAC-SFN/CCM-NPs also exhibited better cytotoxicity effect than that of LAC-SFN-NPs and LAC-CCM-NPs (P < 0.05), which was further analyzed by CI_{50} to confirm the synergism or antagonism effects for these drugs. LAC-SFN/CCM-NPs, SFN/CCM-NPs and free SFN/CCM showed CI_{50} value <1 when the percentage of affected cells was between 20 and 80%, showing the synergy effects of SFN and CCM (Figure 5B).

Cell Uptake

Figure 6 shows that the cell uptake efficiency of LAC-SFN/CCM-NPs was significantly higher than SFN/CCM-NPs (P < 0.05). Cellular uptake efficiency of LAC-SFN/CCM-NPs, LAC-NPs, LAC-SFN-NPs, LAC-CCM-NPs showed no obvious difference compared with each other (P > 0.05).

In vivo Anti-Tumor Efficacy

Tumor volumes of HCC tumor tumor-bearing mice were measured and plotted to evaluate the in vivo anti-tumor efficacy of the nanoparticles (Figure 7A). Blank LAC-NPs could not inhibit the tumor growth. Compared with the control, all drug contained treatment groups significantly inhibited the tumor growth. At the end of the experiment, LAC-SFN/CCM-NPs group exhibited the smallest tumor volume (239 ± 14 mm^3), which is smaller than that of LAC-SFN-NPs group (432 ± 21 mm^3) and SFN/CCM-NPs group (531 ± 29 mm^3) (P < 0.05). The inhibition rate of LAC-SFN/CCM-NPs, LAC-SFN-NPs, LAC-CCM-NPs, SFN/CCM-NPs, and free SFN/CCM groups were 77.4, 59.2, 27.8, 49.9, and 15.3, respectively (Figure 7C). Combine the results of the tumor images (Figure 7B), LAC-SFN/CCM-NPs is the most effective treatment in reducing the tumor volume than non-modified, single drug contained nanoparticles, and free drugs.

In vivo Tissue Distribution

In vivo tissue SFN and CCM distribution in tissues are presented in Figure 8. The SFN and CCM distributions of
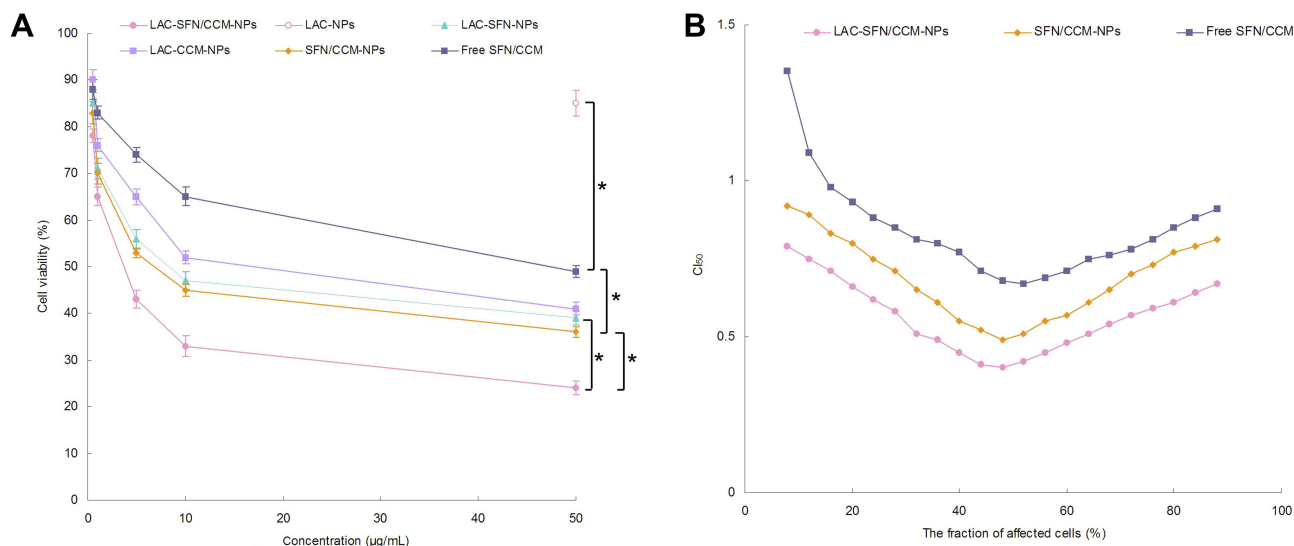
Figure 5 In vitro cytotoxicity of LAC-SFN/CCM-NPs, LAC-NPs, LAC-SFN-NPs, LAC-CCM-NPs, SFN/CCM-NPs, and free SFN/CCM tested on HepG2 cells (**A**) and CI_{50} values investigation (**B**). LAC-SFN/CCM-NPs showed remarkably higher cytotoxicity than SFN/CCM-NPs, LAC-SFN-NPs and LAC-CCM-NPs. CI_{50} value <1 when the percentage of affected cells was between 20 and 80%, showing the synergy effects of SFN and CCM. Data represent mean ± SD, *means $P < 0.05$.
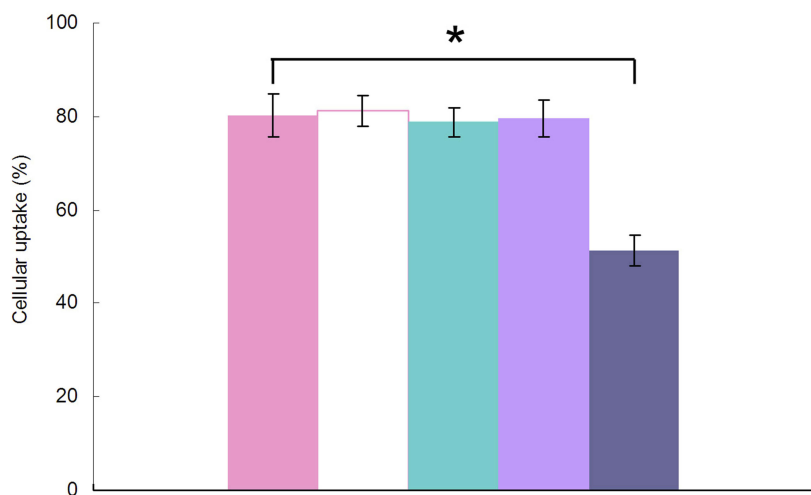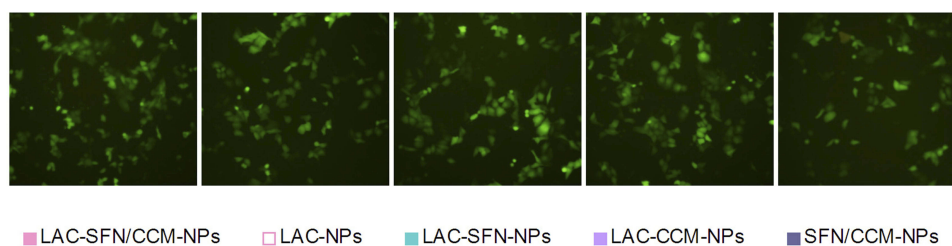

Figure 6 Cellular uptake efficiency of the coumarin 6-loaded nanoparticles in HepG2 cells. Data represent mean ± SD, *means $P < 0.05$.

LAC-SFN/CCM-NPs in tumor and liver were higher than that of SFN/CCM-NPs at 24 h ($P < 0.05$); the latter was higher than free SFN/CCM ($P < 0.05$). On the other hand, SFN and CCM distributions in the hearts and kidneys of mice were reduced when loaded in nanoparticles in comparison with free drugs group.
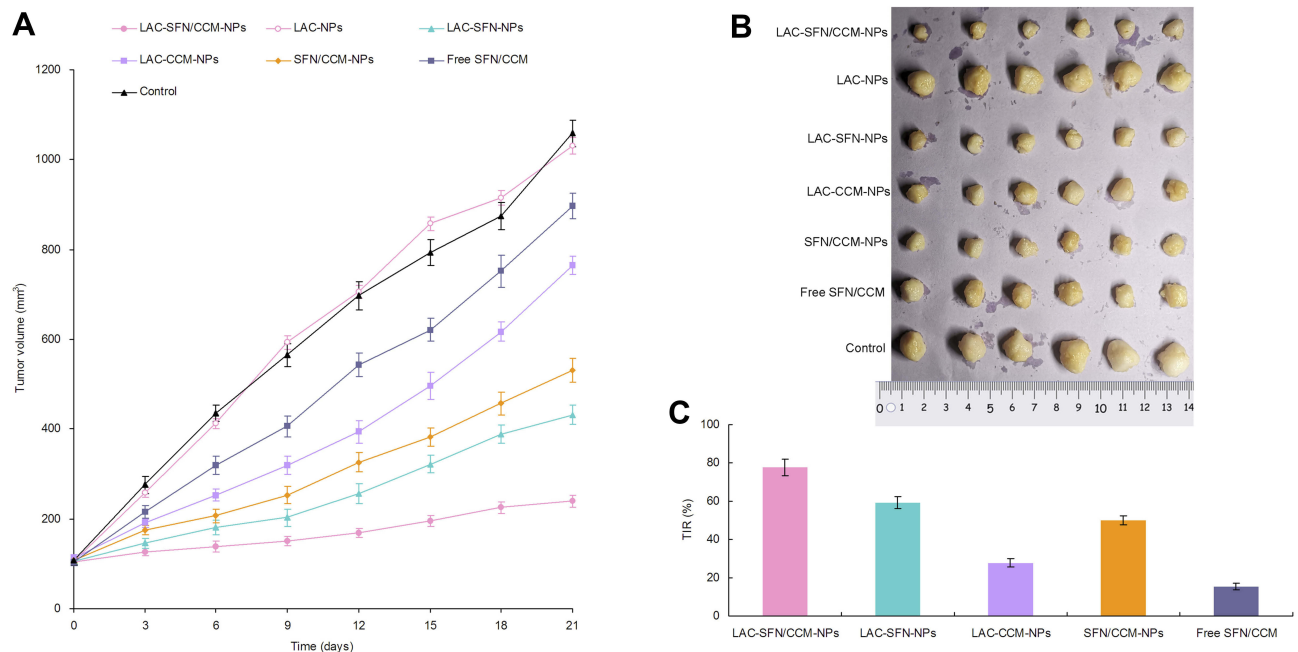
Figure 7 Tumor volumes of HCC tumor tumor-bearing mice (**A**), the tumor images (**B**) and the inhibition rate (**C**). LAC-SFN/CCM-NPs is the most effective treatment in reducing the tumor volume than non-modified, single drug contained nanoparticles, and free drugs.
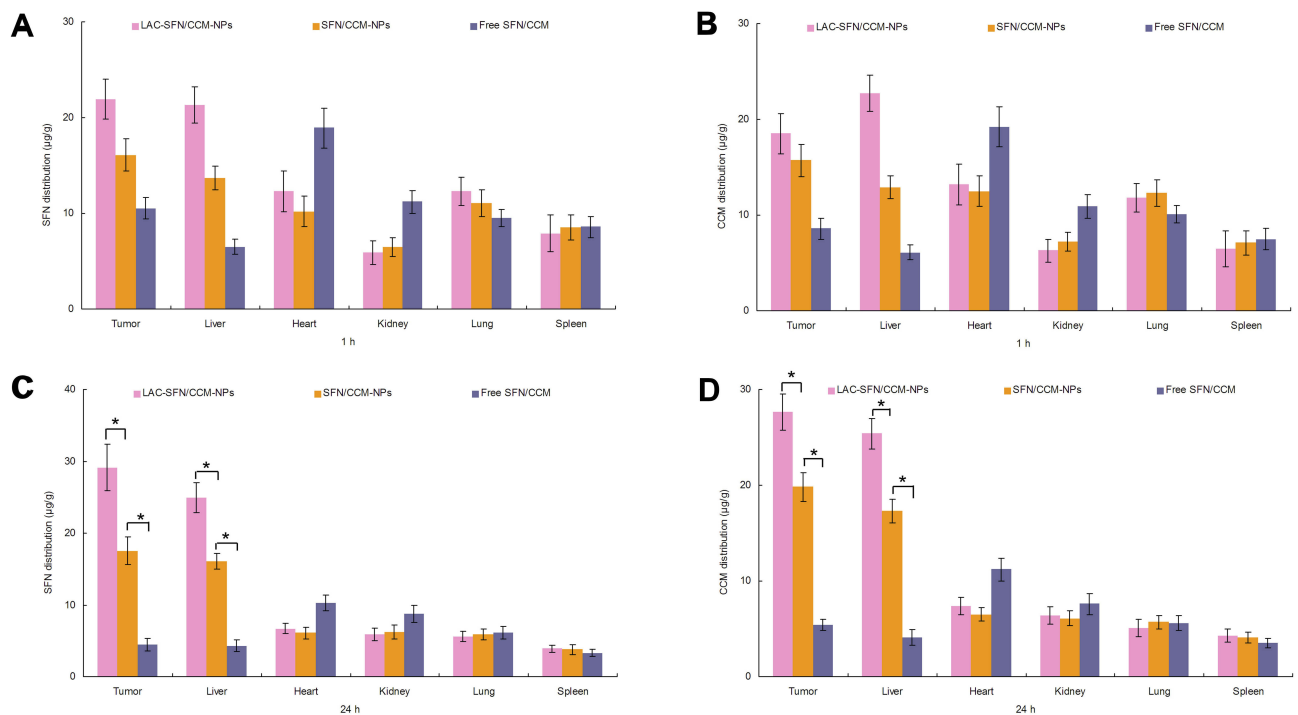

Figure 8 In vivo tissue SFN (**A, C**) and CCM (**B** & (**D**) distribution at 1 and 24 hrs. The SFN and CCM distributions of LAC-SFN/CCM-NPs in tumor and liver were higher than that of SFN/CCM-NPs and free SFN/CCM. Data represent mean ± SD, *means P < 0.05.

In vivo Tolerance Analysis

Blood samples of mice were analyzed to determine the tolerance of nanoparticles in vivo (Figure 9). Free SFN/ CCM induced increasing ALT, CPK, and LDH levels compared with those treated with the control group (P < 0.05). In contrast, the mice treated with LAC-SFN/CCM-NPs and
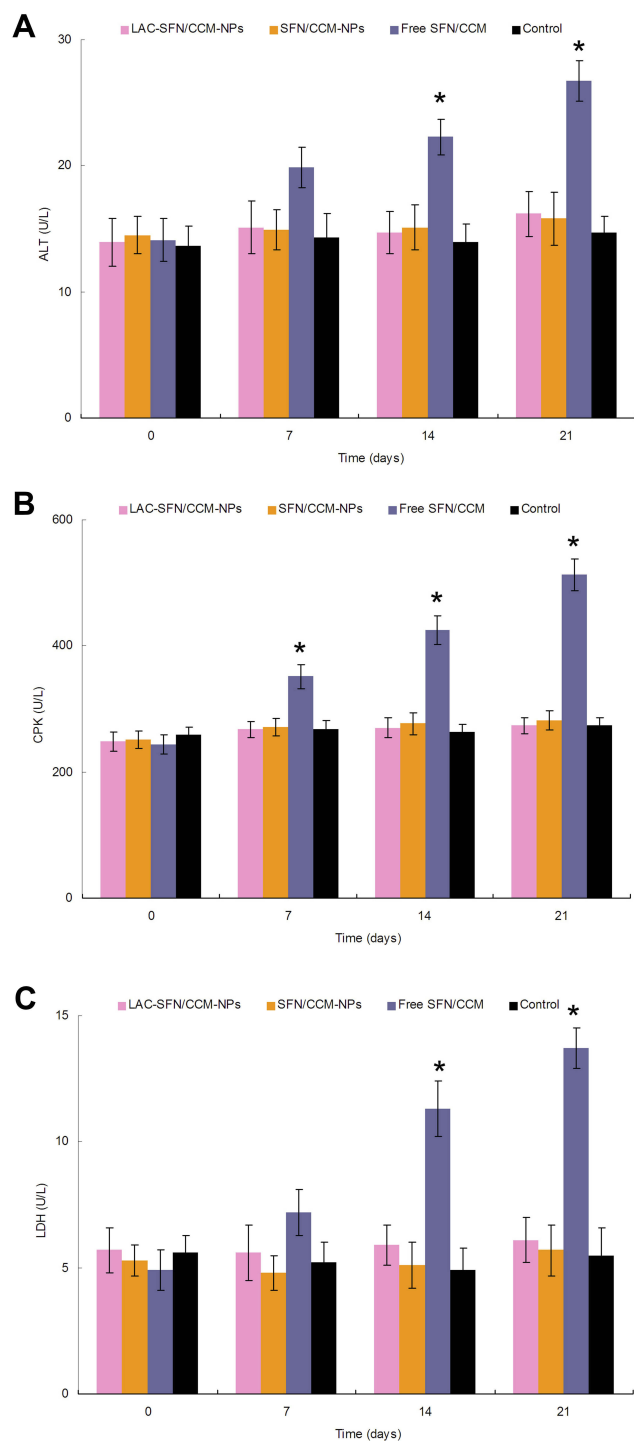
Figure 9 ALT (**A**), CPK (**B**), and LDH (**C**) levels of mice analyzed to determine the tolerance of nanoparticles in vivo. Mice treated with LAC-SFN/CCM-NPs and SFN/CCM-NPs showed a negligible change of those enzymes and markers over the control group. Data represent mean ± SD, *means $P < 0.05$ compared with control.

SFN/CCM-NPs showed a negligible change of those enzymes and markers over the control group. These results indicated that nanoparticles were well tolerated at the tested dose, may not bring side effects and toxicity.

Discussion

To increase the targeted therapy efficiency for HCC, a pH-responsive lactosylated material was first designed and introduced to the formulation. Mammalian hepatic parenchymal cells and HCC cells are known for their highly specific expression of ASGPR on the surface of cell membranes. These receptors are capable of binding galactose moieties and internalize them through receptor-mediated endocytosis.[49] In this section, Lactobionic acid LAC-ADH-PEG-PCL was employed as the recognition moiety to ASGPR, and was attached to PEG-PCL through a pH-responsive ADH bond. According to the CI_{50} values, the minimum value was achieved at the SFN to CCM ratio of 1:1 (w/w). So 1:1 was determined as the drugs ratio to prepare the nanoparticles. The interaction force existed in the LAC-SFN/CCM-NPs may be hydrophobic interactions. Compared with the uniform particles of SFN/CCM-NPs, LAC-SFN/CCM-NPs are spherical particles with light coats on the surface, which could be the evidence of the lactose moiety presented on the surface of the nanoparticles.[50] The size of the LAC-SFN/CCM-NPs was 115.5 ± 3.6 nm, with a PDI of 0.183 ± 0.009. PDI was applied to determine the size range and size distribution of the nanoparticles. For polymer-based nanoparticles, PDI values <0.2 are considered to have a narrow distribution.[51] Zeta potential of nanoparticles was negative, which could reduce clearance by the reticuloendothelial system (RES) due to the low absorption of plasma proteins.[52] The stability of any nanoparticle system needs to be evaluated and optimized, as disruption of the nanoparticles in the drug delivery system may affect its therapeutic potential.[53] No obvious changes in size, PDI, and EE of nanoparticles were found during 6 months of study, which could prove the good stability of the system.

The drug release from nanoparticles was investigated by quantifying the drug amounts in the presence of different pH media.[54] Compared with less than 60% of drug release obtained at pH 7.4, cumulative release of SFN and CCM from nanoparticles at pH 5.5 was over 80%, indicating comparative stability in neutral conditions.[55] The release rate was dramatically improved due to hydrolysis of hydrazone, accelerating the drug release at decreasing pH values, consistent with large numbers of recent studies in pH-responsive drug delivery system.[15,16]

The cytotoxicity data showed that the LAC-SFN/CCM-NPs inhibited the viability and proliferation of the cancer cell lines at low concentrations, this means it had the most significant tumor cell inhibition ability. Higher toxicity of LAC-SFN/CCM-NPs in comparison with SFN/CCM-NPs

may be the evidence of the targeted ability of lactose to cancer cells enhanced the efficiency of the anticancer drugs.[56] LAC-SFN/CCM-NPs and SFN/CCM-NPs showed significantly higher cytotoxicity than free SFN/CCM, which may be explained by the protection effect of nanoparticles thus let the drugs continuously accumulated within the tumor cells and kill them.[57] To understand the effect of dual drugs on cytotoxicity in HepG2 cells, the Chou and Talalay method was used to determine whether the drug combination effect was synergistic, additive, or antagonistic.[20] CI_{50} value of the LAC-SFN/CCM-NPs was the lowest, indicating co-delivery of SFN and CCM by LAC-SFN/CCM-NPs had evident superiority as compared with non-modified SFN/CCM-NPs and free SFN/CCM.

In vivo antitumor efficiency of LAC-SFN/CCM-NPs was better than non-modified SFN/CCM-NPs, which is related to the targeted ability of lactose and the efficiency of the pH-responsive ligands that promote more release of drug in the acidic tumor site.[58,59] Superior tumor inhibition of LAC-SFN/CCM-NPs than single-drug-loaded LAC-SFN-NPs and LAC-CCM-NPs could be due to the synergism effect between SFN and CCM as studied in vitro.[60] In vivo drug distribution of nanoparticles was higher in the tumor tissue and lower in heart and kidney, which could decrease the side effects during the tumor therapy.[61] The SFN and CCM distributions of LAC-SFN/CCM-NPs in tumor and liver were higher than that of SFN/CCM-NPs and free SFN/CCM, indicating the high liver and tumor targeted ability which is important for the HCC treatment. In vivo blood analysis was performed to analyze the clinical chemical parameters.[62] The mice treated with LAC-SFN/CCM-NPs and SFN/CCM-NPs showed a negligible change of those enzymes and markers over the control group, while Free SFN/CCM induced higher ALT, CPK, and LDH. These results indicated that nanoparticles were well tolerated at the tested dose, may not bring side effects and toxicity.

Conclusion

In the present investigation, pH-responsive lactosylated materials were synthesized. LAC-SFN/CCM-NPs were self-assembled by using the nanoprecipitation technique. LAC-SFN/CCM-NPs exhibited the highest tumor inhibition ability but low systemic toxicity. LAC-SFN/CCM-NPs can be considered as a promising system for targeted HCC therapy.

Acknowledgments

Disclosure

The authors report no conflicts of interest in this work.

References

1. Hartke J, Johnson M, Ghabril M. The diagnosis and treatment of hepatocellular carcinoma. *Semin Diagn Pathol*. 2017;34(2):153–159. doi:10.1053/j.semdp.2016.12.011
2. Grandhi MS, Kim AK, Ronnekleiv-Kelly SM, Kamel IR, Ghasebeh MA, Pawlik TM. Hepatocellular carcinoma: from diagnosis to treatment. *Surg Oncol*. 2016;25(2):74–85. doi:10.1016/j.suronc.2016.03.002
3. Kalyan A, Nimeiri H, Kulik L. Systemic therapy of hepatocellular carcinoma: current and promising. *Clin Liver Dis*. 2015;19(2):421–432. doi:10.1016/j.cld.2015.01.009
4. Chong DQ, Tan IB, Choo SP, Toh HC. The evolving landscape of therapeutic drug development for hepatocellular carcinoma. *Contemp Clin Trials*. 2013;36(2):605–615. doi:10.1016/j.cct.2013.03.013
5. Zhu AX. Molecularly targeted therapy for advanced hepatocellular carcinoma in 2012: current status and future perspectives. *Semin Oncol*. 2012;39(4):493–502. doi:10.1053/j.seminoncol.2012.05.014
6. Méndez-Blanco C, Fondevila F, García-Palomo A, González-Gallego J, Mauriz JL. Sorafenib resistance in hepatocarcinoma: role of hypoxia-inducible factors. *Exp Mol Med*. 2018;50(10):134. doi:10.1038/s12276-018-0159-1
7. Wang C, Su L, Wu C, Wu J, Zhu C, Yuan G. RGD peptide targeted lipid-coated nanoparticles for combinatorial delivery of sorafenib and quercetin against hepatocellular carcinoma. *Drug Dev Ind Pharm*. 2016;42(12):1938–1944. doi:10.1080/03639045.2016.1185435
8. Cao C, Wang Q, Liu Y. Lung cancer combination therapy: doxorubicin and β-elemene co-loaded, pH-sensitive nanostructured lipid carriers. *Drug Des Devel Ther*. 2019;13:1087–1098. doi:10.2147/DDDT.S198003
9. Han Y, Zhang Y, Li D, Chen Y, Sun J, Kong F. Transferrin-modified nanostructured lipid carriers as multifunctional nanomedicine for codelivery of DNA and doxorubicin. *Int J Nanomedicine*. 2014;9:4107–4116. doi:10.2147/IJN.S67770
10. Elnaggar MH, Abushouk AI, Hassan AHE, et al. Nanomedicine as a putative approach for active targeting of hepatocellular carcinoma. *Semin Cancer Biol*. 2019;S1044-579X(19)30225–1.
11. Yu W, Liu C, Liu Y, Zhang N, Xu W. Mannan-modified solid lipid nanoparticles for targeted gene delivery to alveolar macrophages. *Pharm Res*. 2010;27(8):1584–1596. doi:10.1007/s11095-010-0149-z
12. Yu W, Zhang N, Li C. Saccharide modified pharmaceutical nanocarriers for targeted drug and gene delivery. *Curr Pharm Des*. 2009;15(32):3826–3836. doi:10.2174/138161209789649547
13. Thao LQ, Lee C, Kim B, et al. Doxorubicin and paclitaxel co-bound lactosylated albumin nanoparticles having targetability to hepatocellular carcinoma. *Colloids Surf B Biointerfaces*. 2017;152:183–191. doi:10.1016/j.colsurfb.2017.01.017
14. Teran-Saavedra NG, Sarabia-Sainz JA, Silva-Campa E, et al. Lactosylated albumin nanoparticles: potential drug nanovehicles with selective targeting toward an in vitro model of hepatocellular carcinoma. *Molecules*. 2019;24:7. doi:10.3390/molecules24071382
15. Cui T, Zhang S, Sun H. Co-delivery of doxorubicin and pH-sensitive curcumin prodrug by transferrin-targeted nanoparticles for breast cancer treatment. *Oncol Rep*. 2017;37(2):1253–1260. doi:10.3892/or.2017.5345

16. Tan S, Wang G. Redox-responsive and pH-sensitive nanoparticles enhanced stability and anticancer ability of erlotinib to treat lung cancer in vivo. *Drug Des Devel Ther*. 2017;11:3519–3529. doi:10.2147/DDDT

17. Li S, Wang L, Li N, Liu Y, Su H. Combination lung cancer chemotherapy: design of a pH-sensitive transferrin-PEG-Hz-lipid conjugate for the co-delivery of docetaxel and baicalin. *Biomed Pharmacother*. 2017;95:548–555. doi:10.1016/j.biopha.2017.08.090

18. Zhang R, Ru Y, Gao Y, Li J, Mao S. Layer-by-layer nanoparticles co-loading gemcitabine and platinum (IV) prodrugs for synergistic combination therapy of lung cancer. *Drug Des Devel Ther*. 2017;11:2631–2642. doi:10.2147/DDDT

19. Khan MW, Zhao P, Khan A, et al. Synergism of cisplatin-oleanolic acid co-loaded calcium carbonate nanoparticles on hepatocellular carcinoma cells for enhanced apoptosis and reduced hepatotoxicity. *Int J Nanomedicine*. 2019;14:3753–3771. doi:10.2147/IJN.S196651

20. Liu B, Han L, Liu J, Han S, Chen Z, Jiang L. Co-delivery of paclitaxel and TOS-cisplatin via TAT-targeted solid lipid nanoparticles with synergistic antitumor activity against cervical cancer. *Int J Nanomed*. 2017;12:955–968. doi:10.2147/IJN

21. Qiu J, Cai G, Liu X, Ma D. α(v)β(3) integrin receptor specific peptide modified, salvianolic acid B and panax notoginsenoside loaded nanomedicine for the combination therapy of acute myocardial ischemia. *Biomed Pharmacother*. 2017;96:1418–1426. doi:10.1016/j.biopha.2017.10.086

22. Song Z, Shi Y, Han Q, Dai G. Endothelial growth factor receptor-targeted and reactive oxygen species-responsive lung cancer therapy by docetaxel and resveratrol encapsulated lipid-polymer hybrid nanoparticles. *Biomed Pharmacother*. 2018;105:18–26. doi:10.1016/j.biopha.2018.05.095

23. Woo JH, Kim YH, Choi YJ, et al. Molecular mechanisms of curcumin-induced cytotoxicity: induction of apoptosis through generation of reactive oxygen species, down-regulation of Bcl-XL and IAP, the release of cytochrome c and inhibition of Akt. *Carcinogenesis*. 2003;24(7):1199–1208. doi:10.1093/carcin/bgg082

24. Kong ZL, Kuo HP, Johnson A, Wu LC, Chang KLB. Curcumin-loaded mesoporous silica nanoparticles markedly enhanced cytotoxicity in hepatocellular carcinoma cells. *Int J Mol Sci*. 2019;20:12. doi:10.3390/ijms20122918

25. Yousef S, Alsaab HO, Sau S, Iyer AK. Development of asialoglycoprotein receptor directed nanoparticles for selective delivery of curcumin derivative to hepatocellular carcinoma. *Heliyon*. 2018;4(12):e01071. doi:10.1016/j.heliyon.2018.e01071

26. Yan J, Wang Y, Zhang X, Liu S, Tian C, Wang H. Targeted nanomedicine for prostate cancer therapy: docetaxel and curcumin co-encapsulated lipid-polymer hybrid nanoparticles for the enhanced anti-tumor activity in vitro and in vivo. *Drug Deliv*. 2016;23(5):1757–1762. doi:10.3109/10717544.2015.1069423

27. Benizri S, Ferey L, Alies B, et al. Nucleoside-lipid-based nanocarriers for sorafenib delivery. *Nanoscale Res Lett*. 2018;13(1):17. doi:10.1186/s11671-017-2420-2

28. Wang H, Sun S, Zhang Y, et al. Improved drug targeting to liver tumor by sorafenib-loaded folate-decorated bovine serum albumin nanoparticles. *Drug Deliv*. 2019;26(1):89–97. doi:10.1080/10717544.2018.1561766

29. Cao H, Wang Y, He X, et al. Codelivery of sorafenib and curcumin by directed self-assembled nanoparticles enhances therapeutic effect on hepatocellular carcinoma. *Mol Pharm*. 2015;12(3):922–931. doi:10.1021/mp500755j

30. Zheng N, Liu W, Li B, et al. Co-delivery of sorafenib and metapristone encapsulated by CXCR4-targeted PLGA-PEG nanoparticles overcomes hepatocellular carcinoma resistance to sorafenib. *J Exp Clin Cancer Res*. 2019;38(1):232. doi:10.1186/s13046-019-1216-x

31. Zhou X, Zhang M, Yung B, et al. Lactosylated liposomes for targeted delivery of doxorubicin to hepatocellular carcinoma. *Int J Nanomed*. 2012;7:5465–5474. doi:10.2147/IJN.S33965

32. Duhem N, Danhier F, Pourcelle V, et al. Self-assembling doxorubicin-tocopherol succinate prodrug as a new drug delivery system: synthesis, characterization, and in vitro and in vivo anticancer activity. *Bioconjug Chem*. 2014;25(1):72–81. doi:10.1021/bc400326y

33. Park C, Yoo J, Lee D, Jang SY, Kwon S, Koo H. Chlorin e6-loaded PEG-PCL nanoemulsion for photodynamic therapy and in vivo drug delivery. *Int J Mol Sci*. 2019;20:16. doi:10.3390/ijms20163958

34. Zia Q, Khan AA, Swaleha Z, Owais M. Self-assembled amphotericin B-loaded polyglutamic acid nanoparticles: preparation, characterization and in vitro potential against Candida albicans. *Int J Nanomed*. 2015;10:1769–1790. doi:10.2147/IJN.S63155

35. Babos G, Biró E, Meiczinger M, Feczkó T. Dual drug delivery of sorafenib and doxorubicin from PLGA and PEG-PLGA polymeric nanoparticles. *Polymers (Basel)*. 2018;10:8. doi:10.3390/polym10080895

36. Wang W, Chen T, Xu H, et al. Curcumin-loaded solid lipid nanoparticles enhanced anticancer efficiency in breast cancer. *Molecules*. 2018;23:7.

37. Zheng G, Zheng M, Yang B, Fu H, Li Y. Improving breast cancer therapy using doxorubicin loaded solid lipid nanoparticles: synthesis of a novel arginine-glycine-aspartic tripeptide conjugated, pH sensitive lipid and evaluation of the nanomedicine in vitro and in vivo. *Biomed Pharmacother*. 2019;116:109006. doi:10.1016/j.biopha.2019.109006

38. Luo W, Wen G, Yang L, et al. Dual-targeted and pH-sensitive doxorubicin prodrug-microbubble complex with ultrasound for tumor treatment. *Theranostics*. 2017;7(2):452–465. doi:10.7150/thno.16677

39. Zhu B, Yu L, Yue Q. Co-delivery of vincristine and quercetin by nanocarriers for lymphoma combination chemotherapy. *Biomed Pharmacother*. 2017;91:287–294. doi:10.1016/j.biopha.2017.02.112

40. Liu L, Dai H, Wu Y, et al. In vitro and in vivo mechanism of hepatocellular carcinoma inhibition by β-TCP nanoparticles. *Int J Nanomed*. 2019;14:3491–3502. doi:10.2147/IJN.S193192

41. Chou TC. Drug combination studies and their synergy quantification using the Chou-Talalay method. *Cancer Res*. 2010;70(2):440–446. doi:10.1158/0008-5472.CAN-09-1947

42. Yan J, Wang Y, Jia Y, et al. Co-delivery of docetaxel and curcumin prodrug via dual-targeted nanoparticles with synergistic antitumor activity against prostate cancer. *Biomed Pharmacother*. 2017;88:374–383. doi:10.1016/j.biopha.2016.12.138

43. Pang X, Wang T, Jiang D, Mu W, Zhang B, Zhang N. Functionalized docetaxel-loaded lipid-based-nanosuspensions to enhance antitumor efficacy in vivo. *Int J Nanomed*. 2019;14:2543–2555. doi:10.2147/IJN.S191341

44. Liu X, Sun Y, Xu S, et al. Homotypic cell membrane-cloaked biomimetic nanocarrier for the targeted chemotherapy of hepatocellular carcinoma. *Theranostics*. 2019;9(20):5828–5838. doi:10.7150/thno.34837

45. Xie F, RL D, WF H, et al. In vivo antitumor effect of endostatin-loaded chitosan nanoparticles combined with paclitaxel on Lewis lung carcinoma. *Drug Deliv*. 2017;24(1):1410–1418. doi:10.1080/10717544.2017.1378938

46. Chen D, Jiang X, Liu J, Jin X, Zhang C, Ping Q. In vivo evaluation of novel pH-sensitive mPEG-Hz-Chol conjugate in liposomes: pharmacokinetics, tissue distribution, efficacy assessment. *Artif Cells Blood Substit Immobil Biotechnol*. 2010;38(3):136–142. doi:10.3109/10731191003685481

47. Zhang Y, Yang C, Wang W, et al. Co-delivery of doxorubicin and curcumin by pH-sensitive prodrug nanoparticle for combination therapy of cancer. *Sci Rep*. 2016;6:21225. doi:10.1038/srep21225

48. Wang G, Wang Z, Li C, et al. RGD peptide-modified, paclitaxel prodrug-based, dual-drugs loaded, and redox-sensitive lipid-polymer nanoparticles for the enhanced lung cancer therapy. *Biomed Pharmacother*. 2018;106:275–284. doi:10.1016/j.biopha.2018.06.137

49. Zhang M, Zhou X, Wang B, et al. Lactosylated gramicidin-based lipid nanoparticles (Lac-GLN) for targeted delivery of anti-miR-155 to hepatocellular carcinoma. *J Control Release*. 2013;168(3):251–261. doi:10.1016/j.jconrel.2013.03.020

50. Zhang L, Zhu D, Dong X, et al. Folate-modified lipid-polymer hybrid nanoparticles for targeted paclitaxel delivery. *Int J Nanomed*. 2015;10:2101–2114. doi:10.2147/IJN.S77667

51. Lu G, Cao L, Zhu C, et al. Improving lung cancer treatment: hyaluronic acid-modified and glutathione-responsive amphiphilic TPGS-doxorubicin prodrug-entrapped nanoparticles. *Oncol Rep*. 2019;42(1):361–369. doi:10.3892/or.2019.7139

52. Shang X, Liu Q, Qin T, et al. Fabrication of cRGD-modified reduction-sensitive nanocapsule via pickering emulsion route to facilitate tumor-targeted delivery. *Int J Nanomed*. 2019;14:3361–3373. doi:10.2147/IJN.S202063

53. Shao Y, Luo W, Guo Q, Li X, Zhang Q, Li J. In vitro and in vivo effect of hyaluronic acid modified, doxorubicin and gallic acid co-delivered lipid-polymeric hybrid nano-system for leukemia therapy. *Drug Des Devel Ther*. 2019;13:2043–2055. doi:10.2147/DDDT.S202818

54. Huang H, Yang DP, Liu M, et al. pH-sensitive Au-BSA-DOX-FA nanocomposites for combined CT imaging and targeted drug delivery. *Int J Nanomed*. 2017;12:2829–2843. doi:10.2147/IJN.S128270

55. Ruan S, Yuan M, Zhang L, et al. Tumor microenvironment sensitive doxorubicin delivery and release to glioma using angiopep-2 decorated gold nanoparticles. *Biomaterials*. 2015;37:425–435. doi:10.1016/j.biomaterials.2014.10.007

56. Xu G, Chen Y, Shan R, Wu X, Chen L. Transferrin and tocopheryl-polyethylene glycol-succinate dual ligands decorated, cisplatin loaded nano-sized system for the treatment of lung cancer. *Biomed Pharmacother*. 2018;99:354–362. doi:10.1016/j.biopha.2018.01.062

57. Mandal D, Kumar Dash S, Das B, et al. Bio-fabricated silver nanoparticles preferentially targets gram positive depending on cell surface charge. *Biomed Pharmacother*. 2016;83:548–558. doi:10.1016/j.biopha.2016.07.011

58. Nazari-Vanani R, Moezi L, Heli H. In vivo evaluation of a self-nanoemulsifying drug delivery system for curcumin. *Biomed Pharmacother*. 2019;Volume 14:715–720. doi:10.1016/j.biopha.2017.01.102

59. Gao Z, Li Z, Yan J, Wang P. Irinotecan and 5-fluorouracil-co-loaded, hyaluronic acid-modified layer-by-layer nanoparticles for targeted gastric carcinoma therapy. *Drug Des Devel Ther*. 2017;11:2595–2604. doi:10.2147/DDDT

60. Cai L, Xu G, Shi C, Guo D, Wang X, Luo J. Telodendrimer nanocarrier for co-delivery of paclitaxel and cisplatin: a synergistic combination nanotherapy for ovarian cancer treatment. *Biomaterials*. 2015;37:456–468. doi:10.1016/j.biomaterials.2014.10.044

61. Yu D, Li W, Zhang Y, Zhang B. Anti-tumor efficiency of paclitaxel and DNA when co-delivered by pH responsive ligand modified nanocarriers for breast cancer treatment. *Biomed Pharmacother*. 2016;83:1428–1435. doi:10.1016/j.biopha.2016.08.061

62. Yang F, Li A, Liu H, Zhang H. Gastric cancer combination therapy: synthesis of a hyaluronic acid and cisplatin containing lipid prodrug coloaded with sorafenib in a nanoparticulate system to exhibit enhanced anticancer efficacy and reduced toxicity. *Drug Des Devel Ther*. 2018;12:3321–3333. doi:10.2147/DDDT